

BIRD STRIKE SIMULATION ON COMPOSITE STRUCTURES

R Vijayakumar*, Kalinga Gulbarga and R Ravindranath

Rotary Wing R&D Centre, Hindustan Aeronautics Limited, Bangalore-560017, India

*Corresponding author E-mail: stress.rwrdc@hal-india.com

Abstract

Bird strike analysis is a common type of analysis done during the design and analysis of rotorcraft. These simulations are done in order to predict whether various designs will pass the necessary certification tests. Significant savings can be achieved by using state-of-art modeling tools capable of predicting the composite structural damage due to impact. However, there is a large variability in composite modeling approaches and complexity of simulation processes to design the sandwich structures of an aircraft. This paper investigates the composite structures modeling for bird strike phenomenon in order to validate available numerical models through full scale tests and simulation tools and also addresses a critical review on analysis techniques. The numerical simulation of various cases of the bird impact on rigid plate including the variation of bird porosity, shape and impact velocity was successfully performed to assess the impact behaviour of soft body projectiles. This paper demonstrates the state-of-the-art bird strike simulation methodology developed and accuracy of modeling approaches available in explicit codes are discussed.

1. INTRODUCTION

Composite materials are characterized by high resistance-to-weight ratios and therefore are widely used in aerospace applications. As classic species of cellular materials, honeycombs have attracted a great deal of attraction due to their outstanding properties, such as a high relative stiffness, strength, good insulation and light weight.

Bird strike incidents are not uncommon and cause significant flight threats to rotorcraft safety. The increasing number of bird-plane high velocity impacts gives rise to new CAE methods to address aircraft safety. European Aviation Safety Agency (EASA) certifies civil aircraft to meet series of minimum standards. The FAA's 14 CFR §29.631 prescribes [1] a bird impact and requires that Category A rotorcraft be capable of continued safe flight and landing after the impact. Category B rotorcraft must be capable of a safe landing after the impact. Compliance must be shown by tests or by analysis based on tests carried out on sufficiently representative structures of similar design. To address these crashworthiness regulatory requirements many aircraft manufacturers are turning to simulation technology in product development. Hindustan Aeronautics limited is continuing to develop a bird strike simulation methodology to predict the structural responses and failure modes for both rotating and non-rotating aircraft structures using explicit finite element codes.

During certification process of Advanced Light Helicopter (ALH), bird strike tests and corresponding

simulation analyses were conducted on various external key components (Figure 1) such as cowling, horizontal stabilizer and end plate which are made of fiber reinforced plastic composites, to further validate the simulation methodology. The performance of these external key components are susceptible to collision under bird strike must be demonstrated and they must maintain their structural integrity.

Bird strike analysis is a common type of analysis done during the design and analysis of composite structures such as cowlings, fuselage panels or empennage. Cowlings on roof structure in most of the rotorcraft are manufactured from fibrous sandwich composites. Cowling refers to the detachable panels with cutouts covering those areas into which access must be gained regularly, such as the transmission system, engine and its accessories. It is designed for suction loads and to provide a smooth airflow over the nacelle by protecting the accessories from damage. The bird strike on forward facing cowling structure needs to be complied by the certification standards for which an attempt is made in the present work.



Figure 1 Advanced Light Helicopter

This paper presents some results of the theoretical study and the numerical simulations of high velocity bird impact on a rigid flat plate. Scope of the present work is to illustrate the finite element modelling of composite structures using the state-of-art modeling tools and gives a very useful approach for modelling soft body impacts by addressing accuracy of numerical bird models. The aim of the present work is to develop reliable improved design tool while decreasing the time and costs involved in the certification process.

Most authors studying bird strike have to be satisfied with using the results given by Wilbeck [2-4] to validate their numerical bird model. Marinko Ugrcic [5] and M-A Lavoie et al. [6] illustrated that bird impacts on rigid targets generated peak pressures independent of bird size and proportional to the square of the impact velocity, resulting in a fluid-like response. Barber et al. [7] showed the time-dependent pressure plots for the impact of birds against a rigid wall. In spite of the limitations of the available experimental data, it is still possible to create a respectably valid numerical bird model based on the material properties and shape of a bird and the general behavior of the pressure through time. The elementary bird strike theory is described in the next section.

2. BIRD STRIKE THEORY

The properties related to the idealized bird are complex and largely unknown, and thus far, have been the subject of numerous research efforts [2-14]. One of the main problems in the bird strike simulation is choosing of a shape, material properties and a simulation approach for an object, which model the bird. The common technique is modeling of the bird as a solid ellipsoid, cylinder or hemispherical ended cylinder. The material properties are usually chosen to be similar to the properties of water. In all the models the bird was represented by an idealized geometry and the material model was defined by an equation-of-state (EOS) to describe the pressure-density relationship in the bird medium. The material model often used referred as elastic-plastic hydrodynamic which was originally developed for ballistic impact in metals. The polynomial EOS, which defines the pressure P in the following, is used in modeling the bird and surrounding air. This polynomial EOS for the bird model corresponds to a hydrodynamic, isotropic and non-viscous constitutive law and is defined as below.

EOS of water and air

The polynomial form is an established approximation of the observed EOS used to describe the pressure-density relationship in bird medium [2] as follows:

$$(1) \quad P = C_0 + C_1\mu + C_2\mu^2 + C_3\mu^3 + (C_4 + C_5\mu + C_6\mu^2)E$$

with a known and negligible initial equilibrium pressure, the values of the coefficients in Eq.1 are given as

C_0 = initial equilibrium pressure, negligible

$$C_1 = \rho_0 c_0^2$$

$$(2) \quad C_2 = (2k-1) C_1$$

$$C_3 = (k-1)(3k-1) C_1$$

$$C_4 = C_5 = C_6 = 0$$

Here, μ is given by $\mu = \rho/\rho_0 - 1$, represents a dimensionless parameter defined in terms of the ratio of current density ρ to initial density ρ_0 and represents the change in density during impact and E - internal energy. $C_0 - C_6$ are material constants. These constants refer to the dynamic behaviour of a bird at impact they are difficult to measure directly and have to be determined indirectly. The approach generally used is to calibrate the material parameters by comparing impact simulation results with the test data. These coefficients are given by expressions based on the initial density ρ_0 (for water $\rho_{0,w} = 1000 \text{ kg/m}^3$, for air $\rho_{0,a} = 1.225 \text{ kg/m}^3$) the speed of sound in the medium c_0 (for the water $c_{0,w} = 1483 \text{ m/s}$ and for the air $c_{0,a} = 342 \text{ m/s}$) and an experimental constant k (for water $k_w = 2.0$ and for the air $k_a = 1.03$). The air is modelled by using the Gamma law of EOS, given from Eq.1, as follows:

$$(3) \quad \begin{aligned} C_4 = C_5 = 0.4 \\ C_0 = C_1 = C_2 = C_3 = C_6 = 0 \end{aligned}$$

Through the definition of density, the pressure volume relationship within the above EOS formulation can be established. A bird undergoing impact at high velocity behaves as a highly deformable projectile where the yield stress is much lower than the sustained stress. Accordingly, the impact can be qualified as a hydrodynamic impact. This, and the fact that the density of flesh is generally close to the density of water, makes it possible for a bird to be considered as a lump of water hitting a target. This is the main assumption leading to the understanding of the behaviour of the bird.

The bird strike has been divided into two stages: the initial shock and the steady flow. The pressure of the initial shock called as Hugoniot pressure (P_{sh}) is given by an equation (4), the pressure of the steady flow called as stagnation pressure (P_{stag}) for an incompressible fluid is calculated according to Bernoulli and is given by equation (5) as below.

$$(4) \quad P_{sh} = \rho_0 V_{sh} V_{im}$$

$$(5) \quad P_{stag} = 0.5 \rho_0 V_{im}^2$$

These two pressures are important because the shock pressure (P_{sh}) gives the maximum possible

value for the impact and the stagnation pressure (P_{stag}) gives the expected reading when the flow stabilizes.

EOS of porous material

The EOS of porous medium is based on the thermodynamic equation that describes the state of matter under a given set of physical conditions. The porous medium requires the elastic bulk modulus and the sound speed of porous to be defined. The sound speed is calculated from Eq. 6

$$(6) \quad c_{por} = (1-z)^m c_{0,w} + z c_{0,a}$$

Where z is porosity and m is exponent

In case of porous material density is calculated from Eq. 7

$$(7) \quad \rho_{porous} = (1-z) \rho_{water} + z \rho_{air}$$

The speed of the elastic wave followed by the small perturbations of the bird body particles is equals to the sound velocity in the fluid:

$$(8) \quad c_E = (K/\rho_0)^{0.5}$$

where as c_E is the sound speed in the fluid and K is the elastic bulk modulus of the fluid.

The values of the variables needed to calculate the stagnation pressure are easily available. In case of compressible porous material, we assume that the increasing factor equals $(1-z)^{-1}$.

$$(9) \quad P_{stag} = (1-z)^{-1} \rho_{porous} * 0.5 v_{im}^2$$

On the other hand, the Hugoniot pressure depends on the impact velocity (V_{im}) and the shock velocity (V_{sh}), which itself also depends on the impact velocity. Moreover, the equation changes whether or not porosity is included, or if the fluid considered is water or a substitute. When the fluid flow reaches a steady state, it is also possible to calculate the pressure distribution along the radius.

The available bird modeling techniques are described in the next section.

3. BIRD MODELLING TECHNIQUES

Since late eighties, explicit FE codes have been used to develop high efficiency bird-proof structures [4]. Nevertheless, the analysis of birdstrike onto compliant structures by means of these codes, which adopt a Lagrangian approach, is particularly troublesome. In fact, after the early instants of the impact, the distortions in the mesh of the bird cause

a loss in accuracy, a reduction in the time-step and, eventually, an error termination of the simulation.

In that, techniques based on Eulerian or Arbitrary Lagrangian Eulerian (ALE) approach seem to have an advantage and, therefore, some explicit FE codes have implemented also an Eulerian or an ALE solver. Drawbacks of these solvers (which eventually limit their use) are: the diffusivity, the lack of sharp boundaries, and the large computational resources necessary to run the analysis.

Recently, solvers based on Smoothed Particle Hydrodynamics (SPH) approach have been developed and implemented in the framework of an explicit FE code to analyze events characterized by large deformations.

4. BIRD IMPACT AGAINST A FLAT PLATE

Finite element models were developed to study the impact properties of a soft body onto a target plate which was assumed to be rigid. The purpose of using a rigid flat plate target is to study the bird substitute with different porosities and assessment by comparing the pressure reading at the centre of a flat rigid plate by theoretical and numerical analysis. Since the body of a bird is mainly composed of water, the average density should be close to that of water. However, taking cavities, bones and different anatomical considerations into account, the averaged density is lower than that of water. This work was taken as reference to create simulations similar to those presented [5, 6] earlier.

The substitute bird was developed using two main modeling methods are currently available are considered in the analysis [6]. The simulation technique can be chosen from these methods. The analysis is carried out by Autodyn solver for the simulations but can be done with similar dynamic finite element analysis solvers. At first, a lagrangian approach is adopted with trial and error procedure and then extended to SPH method for avoiding numerical difficulties associated with extensive mesh distortion. The objective of simulation runs is to validate the reliability of various theoretical parameters with the numerical parameters. In all the cases, the substitute birds are fired against an Aluminium alloy (Al 6061T-6) flat plate with dimensions of 0.7x0.7x0.01 m. The flat plate is fixed at all edges. The properties of the Aluminium plate is given in Table 1.

Table 1 Properties of Aluminum Plate

Mass Density, kg/m ³	2700
Young's Modulus, MPa	70000
Poisson's Ratio	0.33

Two typical bird shapes as shown in Fig. 2 are generally used in the bird strike analysis. A cylinder with flat ends or a cylinder with hemispherical ends were considered for the analysis. The properties given in Table 2 along with the length-to-diameter ratio equal to two defines the necessary bird geometry.

For the solid cylinder impactor geometry with a total length equal to twice the diameter, the total volume is given by

$$(10) \quad \text{Volume} = \pi (0.5*D)^2 *L$$

Similarly for a solid cylinder with hemispherical end caps, the total volume is given by

$$(11) \quad \text{Volume} = 0.416*\pi D^3$$

In each case, the height and the diameter of the bird was calculated for the given density and mass of the bird. In all the cases the mass of the bird is assumed as 1.0 kg.

The mechanical properties of the substitute bird depending on an amount of air mixed in, called porosity are given in Table 2.

Table 2 Mechanical properties of the water and the water-air mixture

Porosity (z)	Density, ρ_{porous} kg/m ³	Sound speed, C_{por} (for m=1) m/s	Bulk modulus, K, MPa (for m=1)
0 %	1000.0	1483	2200
10%	900.12	1368	1668
20%	800.25	1256	1260
30%	700.37	1142	907

The hydrodynamic regime was defined by different amounts of EOS corresponding to 0%, 10%, 20% and 30% porosity are studied. The determined relevant mechanical parameters listed in Table 2 are used in the solver P-alpha EOS for the porous material.

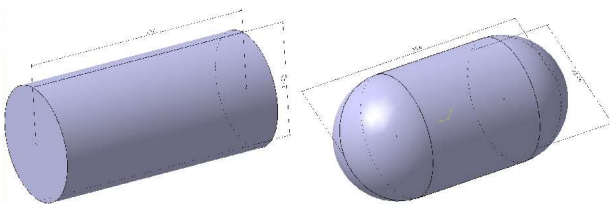


Figure 2 The geometry of dummy bird model

For simplicity, the target structure was assumed to

be rigid for the comparative analysis of the shock pressures and the shock wave velocities. Highly detailed models (Figure 3 and Figure 4) of the bird and the target structure can be built using a variety of spatial discretization modeling approaches.

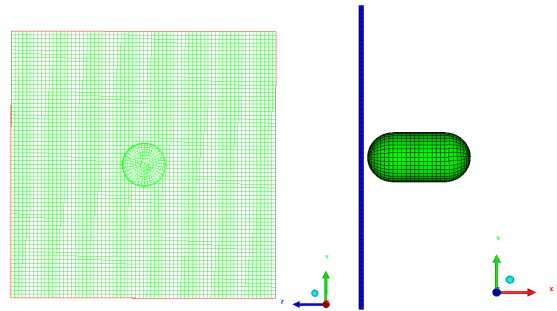


Figure 3 Square rigid plate with Lagrangian bird model

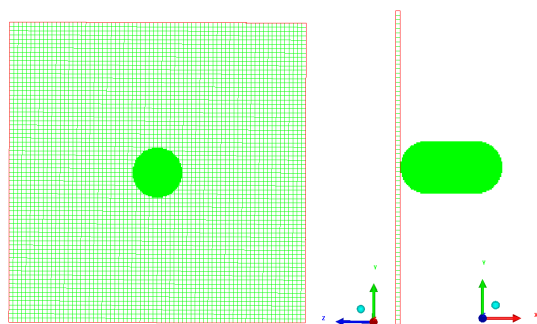


Figure 4 Square rigid plate with SPH bird model

a) Lagrangian Bird Model:

Simulations were performed using an explicit solver Autodyn. The lagrangian method was applied to model bird impacts onto a rigid plate. Figure 5 shows the typical contour plot of four stages; initial impact, shock propagation, steady state flow, and pressure decay phase at varied time intervals. When the bird impacts the target plate, a fragmentation of the projectile particles appears and a shock propagates into the bird. As the shock wave propagates into the bird it brings the bird material behind the shock to rest. The pressure in the shock compressed region is initially very high and uniform across the impact area.

An increase in the number of particles clearly has an influence on the pressure results. The variations of the shock pressure in the water depending on the impact velocity. However, the accuracy of lagrangian bird model results is based on the suitable mesh density and impact velocity of the bird.

At initial impact a shock begins to propagate into the projectile and radial release waves propagate in towards the center from the free surface edges of the projectile. The problem can no longer be

considered to be one-dimensional in nature. For the normal impact of a cylinder, the problem is two-dimensional and axisymmetric. Lagrangian elements for the bird proved unsatisfactory, because the bird behaves hydrodynamically, undergoing severe deformations upon impact. The consequent severe distortions in the lagrangian elements of the bird resulted in several difficulties, such as a necessity for an extremely small time step size and negative element volumes etc. While increasing the density of the mesh one might be able to increase the quality of the pressure results, more mass would be lost, hence never reaching an acceptable result.

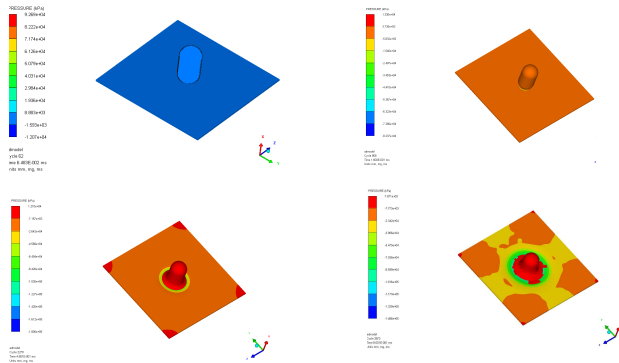


Figure 5 Impact Phases of Substitute bird by Lagrangian approach

b) Smooth Particle Hydrodynamics (SPH) Bird Model:

The impact phases of the selected solutions from SPH method are shown in Figure 6. Analytical results of shock pressure and stagnation are compared from the simulation runs at different time intervals. It is good to notice that the shock pressures are reached simultaneously and that the stagnation pressure is reached at about a second of the simulations.

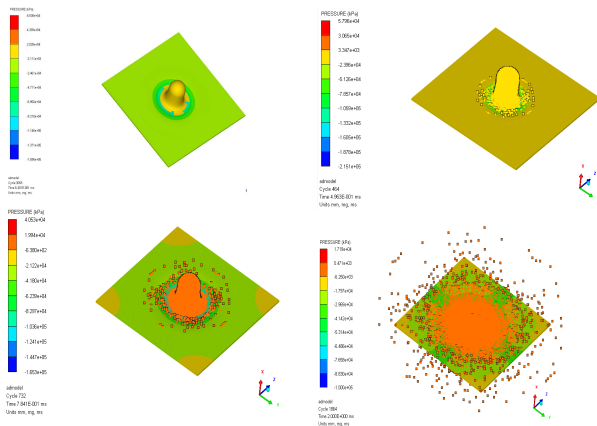


Figure 6 Impact Phases of Substitute bird by SPH approach

Plotting the two different methods together also highlight the fact that the lagrangian model results are much lower than the results of the SPH method. In all the simulations, the impact velocity for all bird projectiles varied from 100 m/s to 500 m/s and was normal to the rigid target. The SPH computed shock pressures for the cylinder with hemispherical bird shape are for an appropriate range of projectile velocities and porosity and compared with the computed shock pressures based on Wilbeck's theory [4].

The analysis of shock pressures calculated on the basis of the hydrodynamic theory and the SPH method shows a good correlation of the computed data, especially for lower values of impact velocities ($V_{im} < 300$ m/s). Further increasing of impact velocity causes a higher deviation of the computed shock pressures.

A homogeneous water-air mixture was used for the bird material and the equation for the elastic bulk modulus and the sound speed of porous medium depending on porosity was involved in the analysis. A simplified shock pressure distribution is used to determine the stagnation pressure in the steady flow regime. The computed stagnation pressures in the steady state regime, calculated by the proposed method, match well with the numerical results.

Previous analyses [5,6] were capable of predicting the steady state stagnation pressure with good accuracy and the shock velocity and the shock pressure are plotted [5] for four different porosities ($z=0.1$ to 0.4) in order to illustrate the influence of that parameter. The steady-state flow pressure stage is considered to be more critical for bird impact events. In fact, Wilbeck's one dimensional theory [2] provides a quick way of checking the steady state pressure before performing a full numerical three-dimensional analysis. After comparing some results of the numerical simulation and the experimental testing, it appears that increasing the porosity might produce a better match of the predicted Hugoniot shock and the FEM pressures with those observed in the experiments.

In addition, the computed stagnation pressures in the steady state regime, calculated by the proposed method, match well with the experimental results. Regarding the shape, it can be seen that the predicted shock pressures associated with all bird shapes produced a good correlation with the experimental results.

The bird models validated by the benchmark problem are adopted in the next section to perform multiple analytical correlation cases on cowling structure.

5. MODELLING OF COMPOSITE STRUCTURES

The following sections describe the numerical model that represents the mechanical behavior of composite structure under bird impact.

Firstly, a workflow is presented to demonstrate the steps followed to carry out this simulation. Starting from the CAD model, a finite element model has been generated and explicit dynamic analysis is performed. Assumptions about material modeling as well as material properties are described in the next sections.

5.1 Workflow

The numerical simulation follows the workflow as shown in Figure 7. The pre-processors of Workbench and Geometry Design modeler are used to clean up the geometry, Engineering data is employed to assign the materials and Explicit Dynamics is make use of to mesh and set up the model. The finite element model with complete set up is transformed to Autodyn solver to carry out the bird strike simulation.

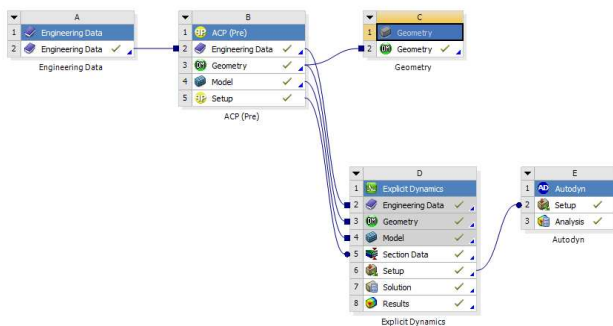


Fig. 7 Work flow of the analysis

5.2 Geometry Model

The imported CAD geometry of the cowling from the Team centre Engineering (TcE) is represented as 3D solid model. The surfaces have been extracted from the solid faces to represent a shell model. The surface model for the purpose of generating Element Sets is shown in Figure 8. Based on the CAD model the mesh was generated in the form of Element Sets.

The cowling is made of light weight sandwich composite structure consisting of kevlar fiber skins and nomex honeycomb core. To represent this sandwich composite structure a shell approach is used that consists in using shell elements for the face sheets as well as honeycomb core. Shell elements account for composite layering with specified laminate definition and failure criteria in order to account damage criteria.

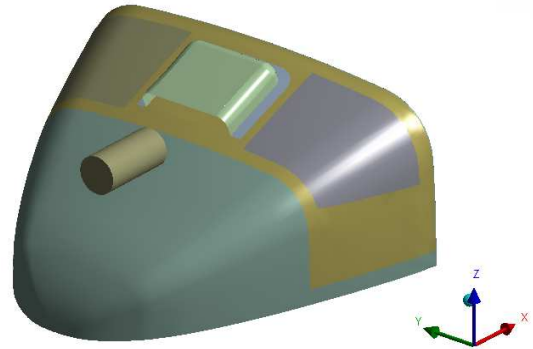


Figure 8 Surface Model of Cowling

The composite failure model which includes ply damage has been used to predict impact damage in the structure using shell elements.

5.3 Composite Modelling using ACP

ANSYS Composite PrepPost provides all necessary functionalities for the analysis of layered composite structures. It is an add-in to ANSYS Workbench and is integrated with the standard analysis features.

Before we go to ACP, it is necessary to create different named selections inside Workbench Explicit Dynamics that will be imported as Element Sets inside ACP. These Element Sets are used to identify elements that will receive layer data of laminate. The meshed input file (*.k) generated by WB LS-Dyna is imported as Element Sets inside ACP and only surfaces are read.

Inside ACP, the properties of composite skins needed were determined by In-Situ characterization tests are created and assigned to each ply. For the determination of the properties of the core, flat wise compression tests under square specimens were performed, according ASTM Standards. Meshing within ANSYS must be done with care to minimize effort in subsequent steps when editing the *.k file to modify material models, element types, and other part specific commands.

Based on this geometry and a FE mesh, the boundary conditions and composite definitions are applied to the structure in the pre-processing stage. In this mode, all composite definitions can be created and are mapped to the geometry (FE mesh). These composite definitions are transferred to the FE model and the solver input file. Layup Plots controls the thickness and ply angle plots in ACP.

Figure 9 shows the thickness distribution for an entire layup. The angle plot is purely a ply-wise plot and shows the orientation angle of a selected ply. Both plots can display the information for all or a selection of elements through the data scope. Thickness and angle plot for all element sets is predefined as a default. The settings in both plots

are similar. The plot definition for layout plots follows the same definition as for solution plots.

A computational constitutive material model for composite damage is considered to characterize the elastic–brittle behavior. In material modeling, composite layers are defined with constitutive material model inside the Ansys Composite PrepPost (ACP) with appropriate damage initiation criteria and damage evolution. Figure 9 and Figure 10 shows the finite element representations of the cowling developed using available pre-processors.

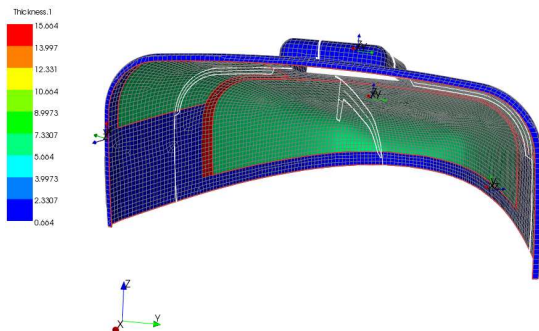
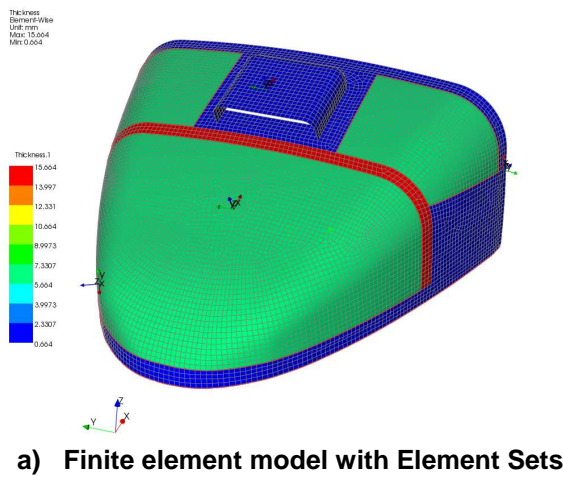


Figure 9 Typical Finite Element Model

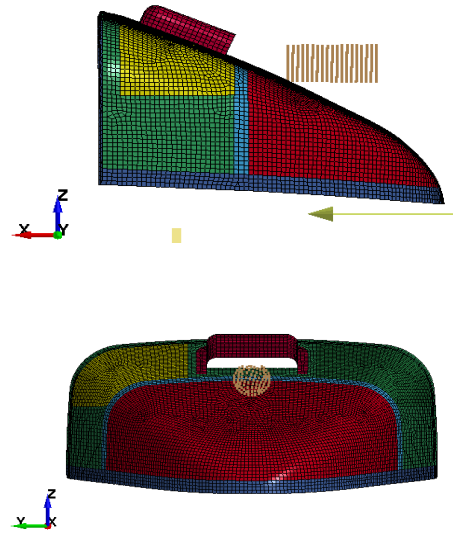


Figure 10 LS DYNA FE model of cowling with SPH bird model

5.4 Material Model

The material model provides a mechanism in an orthotropic material to calculate the contributions to pressure from the isotropic and deviatoric strain components the contributions to the deviatoric stress from the deviatoric strains. Further, this methodology gives rise to the possibility for incorporating nonlinear effects (such as shock effects) that can be attributed to the volumetric straining in the material. To use this model 'Ortho' is selected as the equation state for the material and either 'Polynomial' or 'Shock' for the volumetric response option.

The incremental linear elastic constitutive relations for an orthotropic material can be expressed, in contracted notation, as:

$$(12) \quad \begin{bmatrix} \Delta\sigma_{11} \\ \Delta\sigma_{22} \\ \Delta\sigma_{33} \\ \Delta\sigma_{23} \\ \Delta\sigma_{31} \\ \Delta\sigma_{12} \end{bmatrix} = \begin{bmatrix} C_{11} & C_{12} & C_{13} & 0 & 0 & 0 \\ C_{12} & C_{22} & C_{23} & 0 & 0 & 0 \\ C_{13} & C_{23} & C_{33} & 0 & 0 & 0 \\ 0 & 0 & 0 & C_{44} & 0 & 0 \\ 0 & 0 & 0 & 0 & C_{55} & 0 \\ 0 & 0 & 0 & 0 & 0 & C_{66} \end{bmatrix} \begin{bmatrix} \Delta\varepsilon_{11} \\ \Delta\varepsilon_{22} \\ \Delta\varepsilon_{33} \\ \Delta\varepsilon_{23} \\ \Delta\varepsilon_{31} \\ \Delta\varepsilon_{12} \end{bmatrix}$$

In order to include non-linear shock effects in the above linear relations, it is first desirable to separate the volumetric (thermodynamic) response of the material from its ability to carry shear loads (strength). To this end, it is convenient to split the strain increments into their average, $v\varepsilon_{ave}$, and deviatoric, $v\varepsilon_{ave}^d$, components.

$$(13) \quad \Delta\varepsilon_{ij} = \Delta\varepsilon_{ij}^d + \Delta\varepsilon_{ave}$$

Now, defining the average direct strain increment, $\Delta\varepsilon_{ave}$, as a third of the trace of the strain tensor,

$$(14) \quad \Delta\varepsilon_{ave} = \frac{1}{3}(\varepsilon_{11} + \varepsilon_{22} + \varepsilon_{33})$$

and assuming, for small strain increments, the volumetric strain increment is defined as

$$(15) \quad \Delta\varepsilon_{vol} \approx \varepsilon_{11} + \varepsilon_{22} + \varepsilon_{33}$$

The total strain increments can be expressed in terms of the volumetric and deviatoric strain increments resulting in the following orthotropic constitutive relation.

$$(16) \quad \begin{bmatrix} \Delta\sigma_{11} \\ \Delta\sigma_{22} \\ \Delta\sigma_{33} \\ \Delta\sigma_{23} \\ \Delta\sigma_{31} \\ \Delta\sigma_{12} \end{bmatrix} = \begin{bmatrix} C_{11} & C_{12} & C_{13} & 0 & 0 & 0 \\ C_{12} & C_{22} & C_{23} & 0 & 0 & 0 \\ C_{13} & C_{23} & C_{33} & 0 & 0 & 0 \\ 0 & 0 & 0 & C_{44} & 0 & 0 \\ 0 & 0 & 0 & 0 & C_{55} & 0 \\ 0 & 0 & 0 & 0 & 0 & C_{66} \end{bmatrix} \begin{bmatrix} \Delta\varepsilon_{11}^d + \frac{1}{3}\Delta\varepsilon_{vol} \\ \Delta\varepsilon_{22}^d + \frac{1}{3}\Delta\varepsilon_{vol} \\ \Delta\varepsilon_{33}^d + \frac{1}{3}\Delta\varepsilon_{vol} \\ \Delta\varepsilon_{23} \\ \Delta\varepsilon_{31} \\ \Delta\varepsilon_{12} \end{bmatrix}$$

If the above relations are expanded and the deviatoric and volumetric terms grouped, the following expressions for the direct stress increments results.

$$(17) \quad \begin{aligned} \Delta\sigma_{11} &= \frac{1}{3}(C_{11} + C_{12} + C_{13})\Delta\varepsilon_{vol} + C_{11}\Delta\varepsilon_{11}^d + C_{12}\Delta\varepsilon_{22}^d + C_{13}\Delta\varepsilon_{33}^d \\ \Delta\sigma_{22} &= \frac{1}{3}(C_{21} + C_{22} + C_{23})\Delta\varepsilon_{vol} + C_{21}\Delta\varepsilon_{11}^d + C_{22}\Delta\varepsilon_{22}^d + C_{23}\Delta\varepsilon_{33}^d \\ \Delta\sigma_{33} &= \frac{1}{3}(C_{31} + C_{32} + C_{33})\Delta\varepsilon_{vol} + C_{31}\Delta\varepsilon_{11}^d + C_{32}\Delta\varepsilon_{22}^d + C_{33}\Delta\varepsilon_{33}^d \end{aligned}$$

To find

the equivalent pressure increment, we first define the pressure as a third of the trace of the stress increment tensor;

$$(18) \quad \Delta P = -\frac{1}{3}(\Delta\sigma_{11} + \Delta\sigma_{22} + \Delta\sigma_{33})$$

A general material model requires equation of state (EOS) that relates stress to deformation and internal energy. The stress tensor may be separated into a uniform hydrostatic pressure (all three normal stresses equal) and a stress deviatoric tensor associated with the resistance of the material to shear distortion. For the kevlar fiber skins In-Situ composite material data is used. EOS and Strength models are available within Autodyn.

5.5 SOLVING MODELS

The developed FE model with set up is transferred from Workbench Explicit dynamics to Autodyn solver through seamless integration. We need to define the time step required for models to run. For LS-DYNA simulation runs we have to export the *.k file from the Workbench LS-DYNA. Once the *.k file has been

modified, the model is ready to solve. Setting the MEMORY option is often necessary for large models.

The time step for models as described above are generally in the range of 1e-6sec. This size of time step allows a complete analysis to run within 1 hour on a 3.33 GHz, 16 GB RAM. Since run times vary inversely to time step size, shell models tend to take less time to solve.

After a completed solution, the post-processing is used to evaluate the performance of the design and laminate. In the case of an insufficient design or material failure, the geometry or laminate has to be modified and the evaluation is repeated.

In the post-processing mode, after a completed solution and the import of the result file(s), post-processing results (failure, safety, strains and stresses) can be evaluated and visualized.

6. HIGH VELOCITY IMPACT BEHAVIOR OF COMPOSITE STRUCTURES

Most studies on high velocity impact behavior of sandwich structures are based on full scale tests. The behavior of a composite skin can be considered lineal elastic until the laminate begins to fail. There are several failure mechanisms in a laminate: matrix cracking, tensile and compressive fiber breakage, delamination etc., which depend of many parameters such as fiber and matrix properties, characteristic of the fiber matrix interface and manufacturing process. The methodologies to model the failure of laminates can be categorized into three groups fracture mechanics, failure criteria, and damage mechanics while in some cases it is possible to combine some of them. Of these, failure criteria have demonstrated to be valid in many studies, both under static and dynamic conditions. There are many different failure criteria in the literature [16]. Although some works apply simple failure criteria, such as Tsai Wu or Maximum Stress criteria to study the energy absorption characteristic of structural elements, it is necessary to consider all failure modes that can appear in the breakage of a laminate. Also the evolution of each failure mode and the relations among them has to be incorporated in the model. Numerous failure criteria which consider several damage mechanisms have been used in the bibliography to analyze the failure of composite structures, such as the Hashin criteria [17], Chang Chang criteria [18], Puck criteria [19], Hou criteria [20] or LaRC criteria [21]. The principle objective of the present work is to provide a numerical procedure that is capable of evaluating damage behavior of sandwich panels after a soft body impact.

This paper describes the results from testing and numerical simulation studies on the bird impact and penetration damage of a sandwich cowling by a substitute bird. The main aim was to prove that a correct mathematical model can yield significant information for the designer to understand the mechanism involved in the low-velocity impact event, prior to conducting tests, and therefore to design an impact-resistant aircraft structure. Part of this work presented is focused on the recent progress on the materials modelling and numerical simulation of low-velocity impact response onto a composite aircraft sandwich panel. It is based on the application of explicit finite element analysis codes to study aircraft sandwich structures behaviour under low-velocity impact conditions. Good agreement was obtained between numerical and experimental results, in particular, the numerical simulation was able to predict impact damage and impact energy absorbed by the structure.

For numerical impact analyses of honeycomb sandwich structures, several modelling approaches have been identified. the most widely used approach utilises standard shell finite elements, and is mainly used for approximation of the global behaviour in thin sandwich structures [16]. However, the influence of the honeycomb core inside a sandwich is not yet well known because there is a lack of studies on modelling the behaviour of honeycomb sandwich panels under high velocity impacts. in the present work, a numerical model is used to examine the behaviour of sandwich cowling structure made of kevlar/epoxy laminate skins with nomex honeycomb core under high velocity impacts.

To attain efficiency in numerical analysis, the honeycomb core is usually replaced with an equivalent continuum model. The sandwich structures are analyzed in terms of their effective properties rather than by consideration of their real cellular structure. consequently, the determination of effective elastic properties for this continuum core becomes important.

Honeycomb core under compressive loads behaves elastically at low strains ranging from 0.5 to 5%. Once the stress reaches its yield strength, the progressive core crushing starts at nearly constant stress level called the plateau stress. At a strain value about 85% the stress increases drastically due to mutual pressing of the cell walls. The crushable honeycomb core material model available in ANSYS pre-processor is used to model the nomex core.

Ply Damage Mechanics Model

The failure mechanism of a composite structure under dynamic loads is critical. In the elastic-

damage model of [22] a single composite ply is modelled as a homogeneous orthotropic elastic damaging material whose properties are degraded on loading due to progressive damage processes prior to ultimate failure. The model includes two scalar damage variables: d_2 which quantifies the damage arising from matrix micro-cracking, and d_{12} which relates to fiber/matrix debonding, both of which take on values $0 \leq d_1 \leq 1$.

A plane-stress formulation is adopted and the in-plane stress and elastic strain components are:

$$(19) \quad \boldsymbol{\sigma} = (\sigma_{11}, \sigma_{22}, \sigma_{12})^T$$

$$\boldsymbol{\varepsilon}^e = (\varepsilon_{11}^e, \varepsilon_{22}^e, \gamma_{12}^e)^T$$

The damaged elastic compliance matrix is then written as:

$$(20) \quad \mathbf{S} = \begin{bmatrix} \frac{1}{E_1} & \frac{-\nu_{12}}{E_1} & 0 \\ \frac{-\nu_{12}}{E_1} & \frac{1}{E_2(1-d_2)} & 0 \\ 0 & 0 & \frac{1}{G_{12}(1-d_{12})} \end{bmatrix}$$

where subscripts 1 and 2 denote the fiber and transverse directions, respectively, E_1 , E_2 , G_{12} , and ν_{12} are the elastic properties of the ply, and d_2 and d_{12} are the scalar damage variables describing the loss of rigidity under transverse and shear tension loading, respectively.

The damaged elastic strain energy ($\frac{1}{2}\boldsymbol{\sigma}^T\mathbf{S}\boldsymbol{\sigma}$) is then written as:

$$(21) \quad E_D = \frac{1}{2} \left[\frac{(\sigma_{11})^2}{E_1} - \frac{2\nu_{12}\sigma_{11}\sigma_{22}}{E_1} + \frac{\langle \sigma_{22} \rangle_+^2}{E_2(1-d_2)} + \frac{\langle \sigma_{22} \rangle_-^2}{E_2} + \frac{(\sigma_{12})^2}{G_{12}(1-d_{12})} \right]$$

with

$$\langle a \rangle_+ = a \quad \text{if } a \geq 0; \quad \text{otherwise } \langle a \rangle_+ = 0$$

$$\langle a \rangle_- = a \quad \text{if } a \leq 0; \quad \text{otherwise } \langle a \rangle_- = 0$$

Note that the transverse tension energy and compression energy are split since in compression, microcracks close, so no damage is associated with this loading condition. The elastic damage law is then found from:

$$(22) \quad \boldsymbol{\varepsilon}^e = \frac{\partial E_D}{\partial \boldsymbol{\sigma}} = \mathbf{S}\boldsymbol{\sigma}$$

giving:

$$(23) \quad \varepsilon_{11}^e = \frac{\sigma_{11}}{E_1} - \frac{\nu_{12}\sigma_{22}}{E_1}$$

$$(24) \quad \varepsilon_{22}^e = \frac{\langle \sigma_{22} \rangle_+}{E_2(1-d_2)} + \frac{\langle \sigma_{22} \rangle_-}{E_2} - \frac{\nu_{12}\sigma_{11}}{E_1}$$

$$(25) \quad \gamma_{12}^e = \frac{\sigma_{12}}{G_{12}(1-d_{12})}$$

7. BIRD STRIKE SIMULATION ON COWLING

The bird strike analysis of cowling was performed, using the bird model developed in the section 4, to assess the ability of the composite structure to absorb an impact and prevent detrimental damage to the systems inside the cowling. The model development is described in section 5. The problem of numerical prediction of bird strike damage on composite made cowling structure at a speed of 75 m/s is attempted to assess the damage behavior. The artificial bird is a 1.0 kg impactor with a cylindrical geometry is considered in the analysis. An approximate aspect ratio (L/D) of 2.0 was used for bird model. The dimensions vary depending on the mass of the bird, and are selected from the test data.

In addition, the bird model is assumed as isotropic, homogeneous and elastic-plastic hydrodynamic. The material properties of the bird were similar to a gelatine material with 90% water and 10% air mixture. The mass of the testing birds played an important role in the computer simulation because the pressure distribution greatly depends on the density of the impacting object. The effect of shear modulus and yield stress is not expected to have a significance influence on the stresses developed during impact, as the elastic region is exceeded. The birds used in the tests weigh about 1 kg and are fired at a velocity of 75 m/s. is equivalent to a kinetic energy of 2812.5 J. To achieve a better simulation of the bird-strike event the density of the computer simulated bird is calculated based on the masses of the tests. Material properties of the bird were defined as elastic-plastic-hydrodynamic with Equation of State (EOS) in the form of third degree polynomial.

Bird strike test is carried out on ALH cowling at gas turbine research establishment (GTRE) test facility as per test parameters based on the requirement of specified regulations. During impact high speed cameras are employed for capturing the bird path and velocity measurement. the purpose of bird simulations is to compare numerical results obtained by using the bird modelling methods with the test results.

The FE model was setup to take off the test conditions of the bird strike test conducted at GTRE.

The bird impactor model and damage modeling approaches have been validated by comparison with full scale test results, while the complete damage prediction procedure has been demonstrated with developed finite element model. The kinetic energy dissipated during impact duration by the substitute projectile with impact velocity 75m/s is given in Figure 11. It can be observed from the analysis, the damage behaviour of test and simulations are in good correlation. Also, the damage prediction was attributed based on the bird mass and velocity from of the test data.

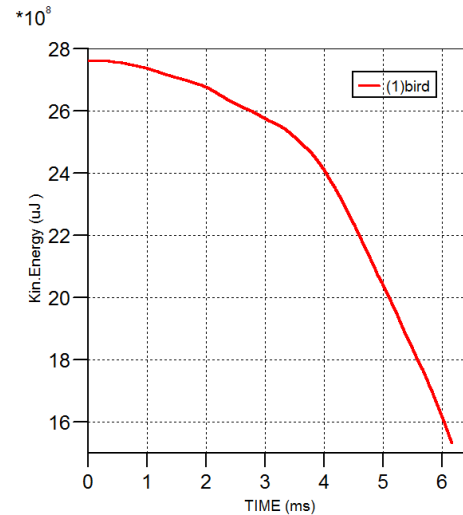


Figure 11 Kinetic Energy plot of the Bird

During impact cowling structure in flight condition is exposed to aerodynamic loads. In order to cover realistic loading conditions of representative structures under bird strike the preload conditions are also included for the compliance of continued safe flight. Lagrangian and SPH bird modelling techniques are employed to simulate the bird strike impacts. SPH bird modeling technique was decided after preliminary simulations carried out with the FE model and verified with the lagrangian bird model. With this configuration the final model had took nearly 1h CPU time for a simulation time of 4000 μ s. Using SPH method, numerous simulations were run with varying number of particles to achieve a better statistical representation of the observed trends from the testing.

Furthermore, the contact algorithm, typically a penalty contact formulation, and its contact stiffness adjustment appear to be one of the key factors on the way to realistic bird strike simulations on composite structures. This model predicts intra-laminar damage modes such as fiber failure in tension and compression, matrix cracking in tension and compression. The damage location, failure size and failure mode of cowling which correlate exponentially well with the test.

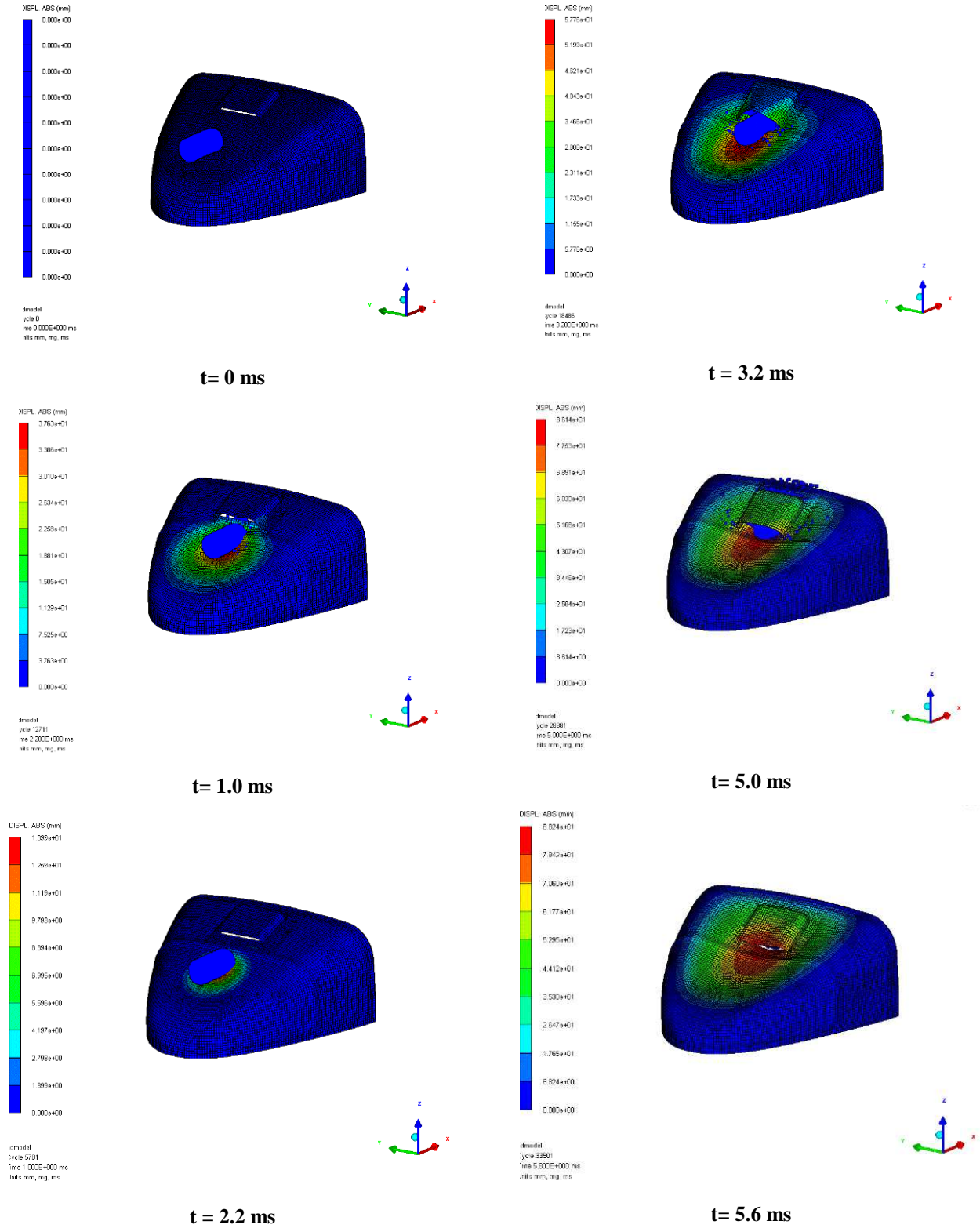


Fig. 12 Deformed plot of cowling at different time intervals

Furthermore, it is clearly visible the deformation of the bird during the impact, and its squashing into the cowling edge is adequately simulated by the present modeling approach.

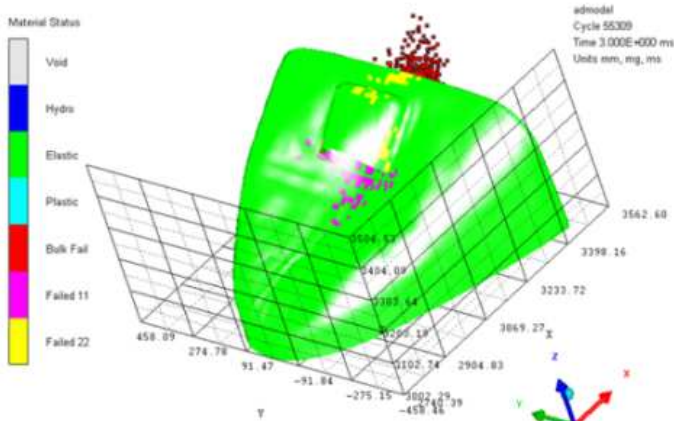


Figure 13 Damage behavior of cowling structure under high velocity impact loading

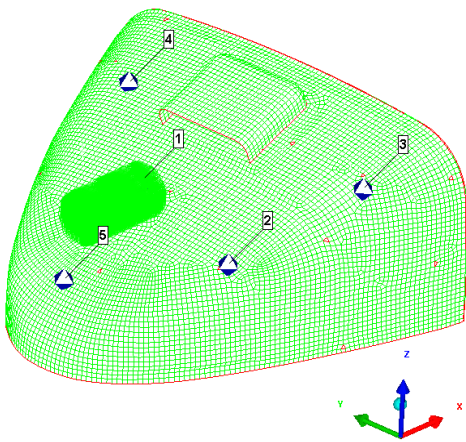


Fig. 14 Cowling structure with specified gauges

The FE model was setup to take off the test conditions of the bird strike test conducted at GTRE. During impact, the cowling structure in flight condition is exposed to aerodynamic loads. In order to cover realistic loading conditions of representative structures under bird strike the preloaded conditions are also included for the compliance of continued safe flight. The damage location, failure size and failure mode with different time intervals from SPH technique is given in Fig. 12 which correlate exponentially well with the test. Fig. 14 shows the cowling structure with specified gauge locations.

The results of bird strike simulation on cowling for the interval of time 3ms are obtained and the tendencies on the damage behaviour of the computer simulations (Fig.13) are compared against the test data. The correlation study established a high degree of confidence in the analytical capability, in predicting the dynamic responses and structural failures subjected to the high-energy bird strike impacts.

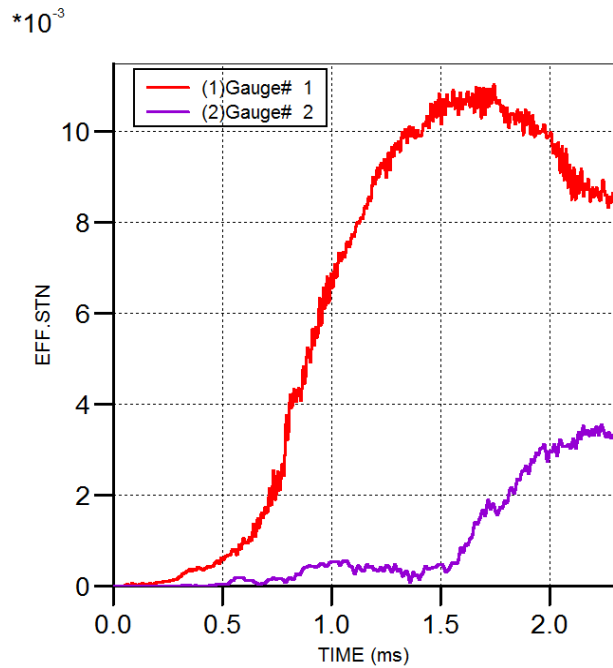


Fig. 15 Effective Strain plot at gauge 1 and 2

The effective strains obtained from the numerical study of the high velocity impact of a soft body projectile on cowling are presented from Fig.15 -17. At the early stages of impact, the mechanical response of the composite structure is controlled by the fiber matrix interface. At the intermediate stages of impact, when the shock wave reaches the face sheet-core interface, a negative-pressure region begins to develop at the back face of the face sheet. This gives rise to the onset of tensile failure of fibres in this region.

At the later stages of impact, a substantially larger region of outer face sheet has been subjected to negative pressures and, consequently, has failed structurally. Meanwhile high strains are observed in the target structure surrounding the tip of the projectile (Fig. 15). Due to high levels of the failure strength/strain of the composite material high pressures do not give rise to significant amount of damage. Composite failure in this region appears to be dominated by the fibre failure mechanism

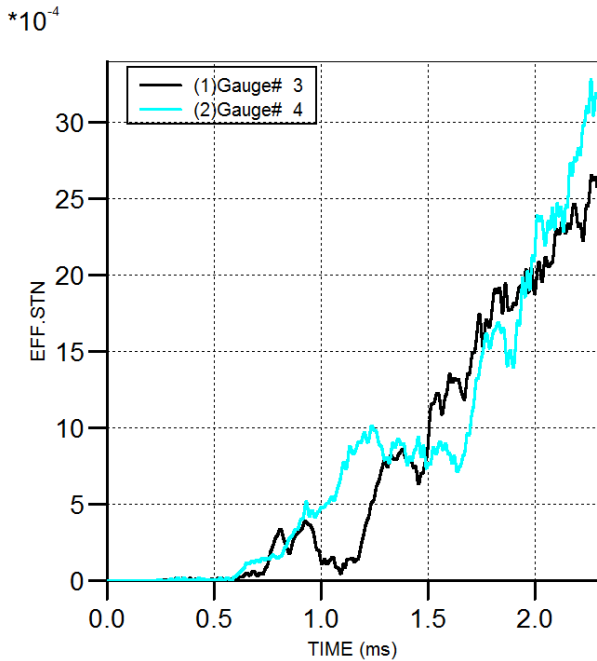


Fig. 16 Effective Strain plot at gauge 3 and 4

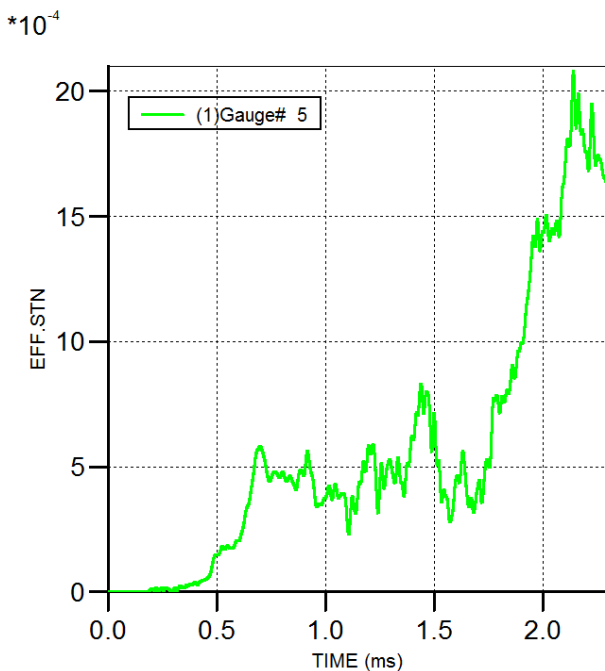


Fig. 17 Effective Strain plot at gauge 5

This complex simulation task in terms of nonlinear composite damage modelling with inter and intralaminar failure modes, implicit-explicit coupling for efficient preload modelling and fluid-structure interaction calculation with hydrodynamic bird impactor models showed that explicit codes are efficient and robust for the prediction of bird impact damage.

8. SUMMARY

In this paper, the composite structures modeling for bird strike phenomenon in order to validate available numerical bird models through full scale tests and simulation tools is addressed. All the calculations carried out in the present work are done using Autodyn, a general purpose non-linear dynamics modeling and simulation software [22]. At first stage, bird strike simulations attempted on a rigid plate using the available bird modeling techniques with influencing parameters to investigate the effect of porosity. The work is based on the application of explicit dynamic analysis to simulate the response of composite structures under soft body impact loads. In the second stage, an improved finite element model of cowling under bird strike loading was attempted using state-of-art composite modelling tools. The results obtained using this model were compared against the test results in terms of damage behaviour and strain data. The validated analytical tool has been successfully used as a design tool to guide the interim design for composite structures.

ACKNOWLEDGMENTS

The design of test fixture and fabrication of test specimens were done in Hindustan Aeronautics Limited. Test support from the design, analysis and testing team of HAL is gratefully acknowledged. The support of the SIMA group at GTRE in carrying out the bird strike tests is also gratefully acknowledged.

REFERENCES

- [1] Policy Statement Number ANE-2001-35 13-R0 *Policy for Bird strike*, Federal Aviation Administration, U.S. Department of Transportation.
- [2] James S Wilbeck, "*Impact behavior of Low Strength Projectiles*", Air Force Materials Laboratory, Technical Report AFML-TR-77-134, 1977.
- [3] James S Wilbeck, James L Rand, "*The Development of a Substitute Bird Model*", *Journal of Engineering for Power*, 1981.
- [4] Wilbeck, J.S. "*Impact behavior of Low Strength Projectiles*". University of Dayton Research Institute for the Airforce Flight Dynamics Laboratory, Wright-Patterson Airforce Base, OH. Technical Report AFML-TR-77-134, 1978.
- [5] Marinko Ugric, "*Application of the Hydrodynamic theory and the Finite element Method in the analysis of Bird Strike in a Flat Barrier*", *Scientific Technical Review*, 2012, Vol. 62, No 3-4 pp. 28-37.

- [6] M-A Lavoie, A. Gakwaya, M. Nejad Ensan and D.G. Zimcik., "Validation of Available Approaches for Numerical Bird Strike Modeling Tools", International Review of Mechanical Engineering (I.RE.M.E.), May 2007.
- [7] J. P. Barber, H. R. Taylor, J. S. Wilbeck, "Characterization of Bird Impacts on a Rigid Plate: Part 1", Technical report AFFDL-TR-75-5, Air Force Flight Dynamics Laboratory, Wright-Patterson Air Force Base, OH (1975).
- [8] Sebastian Heimbs "Computational methods for bird strike simulations: a review" Computers & Structures, Volume 89, Issues 23–24, December 2011, Pages 2093-2112.
- [9] Sebastian Heimbs, "Bird Strike Simulations on Composite Aircraft Structures" 2011 SIMULIA Customer Conference.
- [10] Lavoie M.A., Gakwaya, A, Ensa, M.N., Zimcik, D.G., "Review of existing numerical methods and validation procedure available for bird strike modeling, International conference on Computational & Experimental Engineering and Sciences", 2007, pp111-118.
- [11] Heimbs, S., "Bird Strike Analysis in Aircraft Engineering: An Overview", In: *Advances in Mechanical Engineering Research*, Volume 3, D.E. Malach (ed.), Nova Science Publishers, New York, 2011.
- [12] R. Vijayakumar, "Strength Prediction and Bird Strike Simulation of Composite Structures", International conference on Mechanics of Composites, MechComp2014, New York, USA, June 8-12, 2014.
- [13] Vignjevic R, Maengo M., "Modelling of High Velocity Impact on Carbon Fibre Composite Materials, Scientific Technical Review", ISSN 1820-0206, 2010, Vol. 60, No.3-4, pp.3-8.
- [14] Nizampatman, L.S., "Models and methods for bird strike load predictions", PhD Dissertation, Faculty of Graduate School, Wichita State University, USA, (2007).
- [15] Meo M, Morris AJ, Vignjevic R, Marengo G. "Numerical simulation of low-velocity impact on an aircraft sandwich panel", *Compos Struct* 2003;62:353–60.
- [16] Paris F. "A study of failure criteria of failure of fibrous composite materials". NASA/CR-2001-210661; 2001.
- [17] Hashin Z, Rotem A. "Fatigue criterion for fiber-reinforced materials". *J Compos Mater* 1973;7:448–64.
- [18] Chang F, Chang K. "A progressive damage model for laminated composites containing stress concentrations". *J Compos Mater* 1987;21:834–55.
- [19] Puck A, Schurmann H. "Failure analysis of FRP laminates by means of physically based phenomenological models". *Compos Sci Technol* 1998;58:1045–67.
- [20] Hou JP, Petrinic N, Ruiz C, Hallett SR. "Prediction of impact damage in composite plates". *Compos Sci Technol* 2000;60:273–81.
- [21] Davila CG, Camanho PP. "Failure criteria for FRP laminates in plane stress". NASA/RM-2003-212663; 2003.
- [22] ANSYS (2010). Ansys User's Manual. ANSYS Inc., Canonsburg, USA.